Solar Energy Materials and Solar Cells 182 (2018) 228–236

Contents lists available at ScienceDirect

Solar Energy Materials and Solar Cells

journal homepage: www.elsevier.com/locate/solmat

Insight into the role of post-annealing in air for high efficient $Cu_2ZnSn(S,Se)_4$ solar cells

Shoushuai Gao[a], Yi Zhang[a,*], Jianping Ao[a,*], Xiuling Li[a], Shuang Qiao[b], Ying Wang[b], Shuping Lin[a], Zhaojing Zhang[a], Dongxiao Wang[a], Zhiqiang Zhou[a], Guozhong Sun[a], Shufang Wang[b], Yun Sun[a]

[a] Institute of Photoelectronic Thin Film Devices and Technology, Tianjin Key Laboratory of Photoelectronic Thin Film Devices and Technology, and Key Laboratory of Optoelectronic Information Technical Science of the Education Ministry of China, Nankai University, Tianjin 300071, PR China
[b] College of Physics Science and Technology, Hebei University, Baoding 071002, PR China

ARTICLE INFO

Keywords:
Kesterite
$Cu_2ZnSn(S,Se)_4$
Solar cells
Post-annealing
Defect
Carrier density

ABSTRACT

The device performance of $Cu_2ZnSn(S,Se)_4$ (CZTSSe) solar cells are improved significantly by annealing the full devices at 270 °C for 3 min in air. This paper proposes the origin of the improvement of solar cell by post-annealing treatment by analyzing the results of external quantum efficiency (EQE), Raman spectra, capacitance-voltage (*C-V*), admittance spectra (AS) measurements, and numerical simulation. The experimental results show that the dominant free hole carriers changed from deep defect Cu_{Zn} to the much higher density of shallow defect V_{Cu} after annealing process, which resulting the increase of density of benign $[V_{Cu} + Zn_{Cu}]$ defect cluster, and the decrease of density of detrimental $[2Cu_{Zn} + Sn_{Zn}]$ defect cluster in the surface region of absorber. As a result, the open voltage (V_{OC}) and fill factor (*FF*) increase significantly. The short circuit current density (J_{SC}) increases slightly, which can be attributed to the decrease of interface recombination as well as the improvement of band alignment at CdS/CZTSSe interface. As a consequence, the conversion efficiency of CZTSSe solar cell is improved from 4.41% to 8.02% by post-annealing the full device. Additionally, numerical simulations using wxAMPS software are conducted to reveal insight into the role of the changes of defect type, defect density, and carrier density by post-annealing treatment.

1. Introduction

In the past several years, kesterite structure $Cu_2ZnSn(S,Se)_4$ (CZTSSe) solar cells have attracted much attention due to the low cost, earth-abundant raw materials, and large potential for high conversion efficiency [1–4]. Although the record efficiency of CZTSSe solar cells have achieved to 12.6%, it is far from its theoretical limits (≈ 30%) and even the record efficiency of 22.6% for its predecessor $Cu(In,Ga)Se_2$ (CIGS) solar cells [5–8]. The key limiting factor for high efficient CZTSSe solar cells is the large open circuit voltage deficit (V_{OC}-deficit), expressed as E_g/q - V_{OC}, where E_g is the energy bandgap and q is the elemental charge. The V_{OC}-deficits for record CIGS and CZTSSe solar cells are 0.4 eV and 0.6 eV, respectively [5,9,10]. It is indicated that the large V_{OC}-deficit can be partially attributed to the electrostatic potential fluctuations and band tails, which are caused by the Cu/Zn disorder [11–16], and the interface recombination, including the unfavorable band alignment and interface defect states [17–19].

Recently, the study of post-annealing CZTSSe absorber or devices has attracted much attention because an order-disorder transition is discovered after low-temperature post-annealing treatment for $Cu_2ZnSnSe_4$ (CZTSe) and Cu_2ZnSnS_4 (CZTS) absorber, respectively [14,20]. Several groups have reported the performance improvement of CZTSSe solar cells after post-annealing treatment [21–28]. For example, IBM group indicated that the efficiency can be improved significantly by annealing the bare CZTSSe absorber at 375 °C in air [22]. The performance improvement is attributed to the formation of a Cu-depleted absorber surface and the passivation of grain boundaries by SnOx after air annealing [22]. Saucedo group in IREC indicated that the post-annealing treatment of the full CZTSe solar cells can promote a more Cu poor and Zn rich absorber surface, which are partly responsible for the improvement of device performance [24,25].

However, the reasons why the device performance is improved by post-annealing treatment are still not clear and still confused. This paper proposes the mechanisms from the point of view of improvement of interface properties and defect states. First, the changes of external quantum efficiency (EQE) response are analyzed in detail in terms of

* Corresponding authors.
E-mail addresses: yizhang@nankai.edu.cn (Y. Zhang), aojp@nankai.edu.cn (J. Ao).

https://doi.org/10.1016/j.solmat.2018.03.029
Received 21 November 2017; Received in revised form 28 February 2018; Accepted 15 March 2018
0927-0248/

Table 1
List of the photovoltaic and diode parameters of as fabricated and annealed CZTSSe solar cells, respectively. Series resistance (R_S), shunt resistance (R_{Sh}), ideality factor (A), and reverse saturation current density (J_0) are fitted based on the light *J-V* curves using the procedure outlined in Ref. [57].

Annealing Temperature	Sample	*Eff* [%]	V_{OC} [mV]	J_{SC} [mA/cm^2]	*FF* [%]	R_S [Ω cm^2]	R_{Sh} [Ω cm^2]	A	J_0 [mA/cm^2]
220 °C	As Fabricated	3.73	352	26.77	39.55	3.95	59.1	2.06	2.9×10^{-2}
	After Annealed	3.27	358	27.86	32.83	8.48	34.4	1.14	1.02×10^{-4}
270 °C	As Fabricated	4.41	358	30.07	40.96	3.77	62.6	1.84	1.3×10^{-2}
	After Annealed	8.02	424	31.69	59.69	1.20	756.7	1.77	2.9×10^{-3}
320 °C	As Fabricated	4.29	346	27.67	44.77	1.85	71.9	2.36	7.8×10^{-2}
	After Annealed	4.34	400	28.14	38.59	6.27	86.9	1.43	5.46×10^{-4}

the changes of bandgap, improvement of band alignment, and reduction of interface recombination. Afterwards, the results from Raman spectra, capacitance-voltage (*C-V*), admittance spectra (AS) measurements indicate that the surface of CZTSSe absorber becomes more Cu-poor and Zn-rich after post-annealing treatment, leading to the dominant free hole carriers changing from deep defect Cu_{Zn} to the much higher density of shallow defect V_{Cu}, the increase of density of benign $[V_{Cu} + Zn_{Cu}]$ defect cluster, and the decrease of density of detrimental $[2Cu_{Zn} + Sn_{Zn}]$ defect cluster in the surface region of absorber after post-annealing treatment. We reveal insight into the role of the improvement of band alignment, interface recombination, defect type, defect density and carrier density on the device performance by numerical simulation using wxAMPS software. As a result, the device performance of CZTSSe solar cell is improved significantly from 4.41% to 8.02% by post-annealing treatment in air.

2. Experimental

Cu_2ZnSnS_4 (CZTS) precursors were prepared by sol-gel method. The precursor solutions and the precursor films were prepared as the methods described in Ref. [29]. Afterwards, the precursor films were selenized to form CZTSSe absorbers at 550 °C for 40 min under Se atmosphere (ca. 10^4 Pa) in a furnace, which was evacuated and refilled with argon gas to a process pressure of (ca. 10^5 Pa).

After that, CZTSSe thin film solar cells were completed by a chemical bath deposited cadmium sulfide buffer layer (CdS, ca. 50 nm), a mid-frequency magnetron sputtered intrinsic zinc oxide window layer (i-ZnO, ca. 50 nm), a DC-magnetron sputtered aluminum-doped zinc oxide transparent conducting layer (ZnO:Al, ca. 500 nm), and an electron beam evaporated Ni/Al grid contact (ca. 2 µm). The active area of each CZTSSe solar cell was about 0.34 cm^2 defined by mechanical scribing. The full CZTSSe solar cells were annealed on a hot plate for 3 min in air to improve the device performance. The experimental results show that 270 °C is the optimum annealing temperature. Thus, if it is not pointed out, the default annealing temperature is 270 °C. ZnO:Al/i-ZnO/CdS/quartz glass and CdS/quartz glass samples were also treated with the same annealing process for the optical characterization before and after annealing process.

The compositions of the CZTS precursors and CZTSSe absorbers were measured by PANalytical MagixPW2403 X-ray fluorescent spectrometer (XRF) calibrated with inductively coupled plasma spectroscopy (ICP) to ensure its accuracy. The CZTSSe absorbers have a Cu-poor and Zn-rich stoichiometry (Cu/(Zn + Sn) = 0.75, Zn/Sn = 1.1), which were measured by XRF. Time-of-flight secondary-ion mass spectrometry (TOF-SIMS) depth profiles were performed using a TOF. SIMS 5–100 instrument by ION-TOF GmbH. Analysis was performed with Bi^+ primary ions with an energy of 60 keV. For sputtering, Cs + ions with an energy of 2 keV were used. The sputtered area was 300 × 300 µm^2, the measurement area was 80 × 80 µm^2 in order to reduce the influence of the crater edge. The photoluminescence (PL) spectra of the solar cells were performed with an optical spectrometer (SP-2500, Princeton Instruments) with an excitation wavelength of 532 nm. The transmittance and reflection spectra were measured by Varian Cary 5000 UV–Vis–NIR Spectrophotometer between 200 and 2000 nm. A Raman spectra (Renishaw Invia) with an excitation wavelength of 785 nm was used to characterize the structure properties and the defect properties of CZTSSe solar cells. The capacitance-voltage (*C-V*) and admittance spectra (AS) measurements were both performed with an HP 4284A LCR meter. The *C-V* data were measured by using 50 mV and 100 kHz alternating current (AC) excitation source with direct current (DC) bias from 0.5 to −1.0 V under dark condition at room temperature. Temperature-dependent AS were measured in the temperature of 120–300 K under dark condition with an AC voltage of 30 mV by varying the frequencies from 25 Hz to 1 MHz. The current density-voltage (*J-V*) characteristics were measured by a solar simulator calibrated with a certified Si solar cell under the standard conditions (AM 1.5 G,1000 W/m^2, 25 °C). The external quantum efficiency (EQE) spectra were measured using a chopped white light source (150 W halogen lamp) calibrated with certified Si solar cell (300–900 nm) and InGaAs solar cell (900–1300 nm). The EQE spectra under dark and under a DC white bias light (300 W/m^2) are measured, respectively.

3. Results and discussion

Table 1 shows the effect of post-annealing treatment in air on the device performance of CZTSSe solar cells. It is obvious that the device performance of as fabricated solar cell is relatively poor, especially low V_{OC} and *FF*. Interestingly, the V_{OC} and *FF* increase significantly and the J_{SC} increases slightly after post-annealing treatment at 270 °C for 3 min in air (shown in Fig. 1). As a consequence, the conversion efficiency increases from 4.41% to 8.02%. However, the conversion efficiency is reduced due to the decrease of *FF* after post-annealing treatment at 220 °C, and the conversion efficiency increases slightly due to the significant increase of V_{OC} and the decrease of *FF* after post-annealing treatment at 320 °C. The experimental results show that 270 °C is the optimum annealing temperature. Thus, we will get insight into the role of the significant improvement of device performance by post-annealing treatment at 270 °C. The following measurements and analyses are made on the CZTSSe solar cells before and after post-annealing treatment at 270 °C.

Fig. 2(a) shows the EQE response of CZTSSe solar cells before and

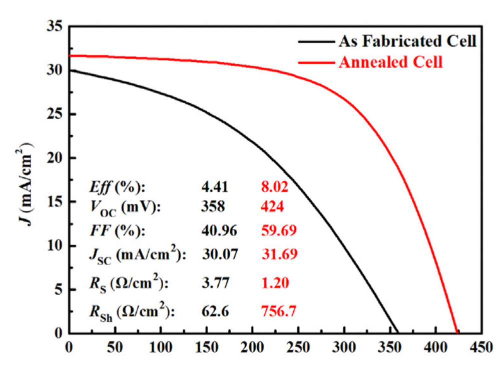

Fig. 1. Current density-voltage (*J-V*) curves and device parameters of as fabricated and annealed CZTSSe solar cells, respectively.